J. Phys. Chem. B **2000,** *104,* 3261−3266 **3261**

Ion-Enhanced Etching of Si(100) with Molecular Chlorine: Neutral and Ionic Product Yields as a Function of Ion Kinetic Energy and Molecular Chlorine Flux[†]

N. Materer,[‡] Rory S. Goodman, and Stephen R. Leone*[,§]

JILA, University of Colorado and National Institute of Standards and Technology, and
Department of Chemistry and Biochemistry, University of Colorado, Boulder, Colorado 80309-0440

Received: September 14, 1999; In Final Form: December 16, 1999

Time-of-flight mass spectrometry (TOFMS) is used to measure neutral and ionic silicon etch products evolved during argon ion-enhanced etching of room temperature Si(100) with molecular chlorine. The yields of these neutral and ionic etch products are examined as a function of ion energy, ion flux, and molecular chlorine flux. For the neutral products, an Ar^+ ion energy range of 275−975 eV is used, while the ionic product measurements are continued down to 60 eV. The atomic Si, SiCl, and $SiCl_2$ neutral etch products are measured without complications due to fragmentation by using 118-nm laser single-photon TOFMS. Atomic Si and SiCl are the major observed etch products. The ionic Si^+ and $SiCl^+$ etch products are also measured using TOFMS; however, the $SiCl_2{}^+$ species is not observed. The similarities between neutral and ionic Si and SiCl etch products as a function of various parameters suggest a model based on direct collisional desorption. For the observed neutral $SiCl_2$ product, the absence of $SiCl_2{}^+$ suggests a different mechanism than that for Si and SiCl. For $SiCl_2$, formation models based on thermal heating or reaction and desorption of neutral species at chemically active surface sites, which are ruled out for Si and SiCl, should be considered.

Introduction

Etching of silicon is a critical manufacturing process in the production of microelectronic devices.[1−3] Etching is generally carried out in halogen-containing plasma environments. In these environments, energetic ion bombardment and reactive gases act in unison to form volatile silicon halide species that desorb from the silicon surface.[1−3] The synergistic action of reactive gases and energetic ions is often termed ion-enhanced etching or reactive ion etching. To produce higher performance devices, more stringent requirements are being placed on the etching process. Objectives such as reduced surface damage and smaller etch features will require additional refinements in current process technologies.

To develop a microscopic understanding of the ion-enhanced etching of silicon, many studies of silicon etching have been performed.[4−11] Recently, studies have been carried out with ion beam energies less than 200 eV.[12,13] From previous investigations, it is generally known that in ion-enhanced etching molecular chlorine chemically affects the substrate by forming new chlorine−silicon bonds and disrupting silicon−silicon bonds.[9] This disruption reduces the total number of chemical bonds that must be broken to collisionally remove silicon-containing species by Ar^+ ion bombardment and increases the total sputtering yield.[9] During ion-enhanced etching, both neutral and ionic etch products are formed. The ionic product must be formed during the energetic impact. In contrast, neutral products can be formed during impact or after impact of the Ar^+ ion due to collisional heating of the surface and at chemically reactive defect sites created by the impact. By comparing neutral to ionic species as a function of bombardment energy and molecular chlorine flux, additional insight into the product formation mechanisms is obtained.

Here we employ time-of-flight mass spectrometry (TOFMS) to study ion-enhanced etching of Si(100) with molecular chlorine. We detect the ionic etch products directly and use single-photon ionization time-of-flight mass spectrometry (SPI-TOFMS) to detect the neutral etch products. The neutral etch products are ionized without dissociation of the neutral parent molecules by using a gentle 118-nm single-photon ionization process.[14] This detection scheme avoids the mass spectral cracking problem normally associated with electron impact ionization. The ability to identify the neutral reaction products allows a direct comparison of the experimental data to molecular dynamics (MD) simulations. In principle at 118 nm, all chlorinated silicon etch products can be detected, with the exception of $SiCl_4$. The lower ionization potential of neutral silicon atoms (Si) as compared to carbon monoxide (CO) and nitrogen (N_2) permits the Si etch product to be detected without interferences by CO and N_2, which have the same mass. SPI-TOFMS has been used to detect Si, SiCl, and $SiCl_2$ cleanly during thermal etching of Si(100)[14] and during ion-enhanced etching[15] with molecular chlorine.

Previous molecular beam studies have examined etch products under ion-enhanced etching conditions.[16−21] These results are summarized in Table 1. Although the etch conditions, chlorine/ion flux ratio, ion identity, and ion energy are similar in the studies mentioned above, there are many discrepancies in these results. Several experimental limitations may contribute to these conflicting results. One problem is related to the use of electron impact ionization for the mass spectrometer detection. In many studies, complex cracking patterns for the etch products are observed, and the actual product distributions have to be inferred. Another difficulty stems from the reactivity of radical etch products. Reactions of these reactive species on the vacuum chamber walls with halogens and other adsorbed species can

---

[†] Part of the special issue "Gabor Somorjai Festschrift".

[‡] Present address, Oklahoma State University, Department of Chemistry.

[§] Quantum Physics Division, National Institute of Standards and Technology.

10.1021/jp993278q CCC: $19.00

TABLE 1: Summary of Previous Experimental Results of Ion-Enhanced Etching of Silicon

study	ion energy (keV)	products[a]	reference
Ar^+, Cl_2	0.275−1	Si, SiCl, ($SiCl_2$)	15
Ar^+, Cl_2	1	$SiCl_2$, $SiCl_4$, (SiCl)	16
Ar^+, Cl_2	0.3−3	$SiCl_4$	18
Ar^+, Cl_2	0.125−0.8	$SiCl_2$, $SiCl_4$	21
Ar^+, Cl_2	1	Si, SiCl, $SiCl_2$	35
Ar^+, Cl_2	3	Si, SiCl, $SiCl_2$	19
Ar^+, Xe^+, Cl_2	0.05−1	SiCl, $SiCl_2$ ($SiCl_3$, $SiCl_4$)	29

[a] Parentheses indicate minor products.

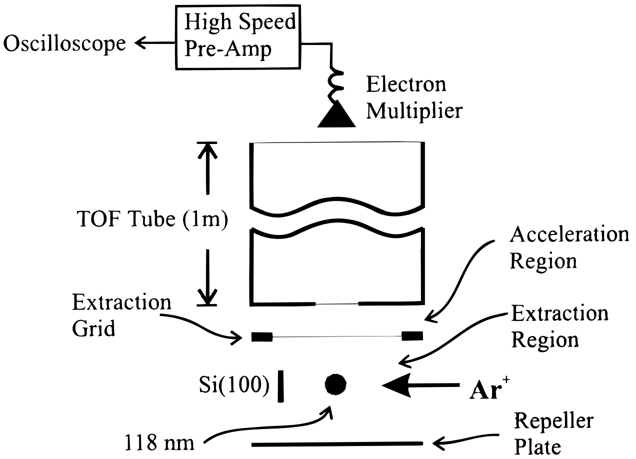

Figure 1. Schematic diagram of the apparatus employed to study ion-enhanced etching. The Wiley−McLaren TOFMS is depicted with separate extraction and acceleration regions. The silicon sample position is indicated relative to the mutually orthogonal, normal incident ion beam, TOFMS flight tube, and 118-nm ionization laser.

obscure the true identities of these products. In previous studies, modulated ion beams were employed to minimize this effect; however, the modulation rates can sometimes be too low to exclude species generated by wall reactions. In contrast, SPI-TOFMS can be used to detect directly the neutral Si, SiCl, and $SiCl_2$ etch products without ambiguity during ion-enhanced etching of silicon with a molecular chlorine background.[15]

Molecular dynamics simulations have also recently elucidated the microscopic mechanisms of ion-enhanced etching of silicon with ion energies below 200 eV.[22−25] Feil et al. examined the formation of surface roughness from chemical sputtering of a chlorinated silicon surface.[23] They observed that chlorine passivation of the surface and the resulting high barriers for surface diffusion resulted in significant surface roughness. Molecular dynamics simulations by Barone et al. using F^+ and Cl^+ ions found a tendency toward less halogenated products with increasing collision energy.[22] Kubota et al. simulated Ar^+-induced etching of clean and chlorinated silicon and reported SiCl as the most abundant product for silicon substrates with an initial chlorine coverage.[24] However, differing amounts of Si and $SiCl_2$ are also found depending on surface disorder and chlorine coverage. In agreement with the study of Kubota et al.,[24] a MD simulation of ion-enhanced etching of silicon with chlorine ions by Hanson et al.[25] indicated that Si, SiCl, and $SiCl_2$ are the main etch products. At the highest energy examined (200 eV), atomic silicon was reported as the most abundant product.[25]

Experimental Section

Figure 1 shows the experimental apparatus[15] used to determine the yields of both neutral and ionic etch products during Ar^+ ion-enhanced etching of a single-crystal Si(100) surface with molecular chlorine. The silicon sample is positioned perpendicular to the flight tube and within the extraction region of a Wiley−McLaren TOFMS.[26] For the neutral products, single-photon ionization at 118 nm (ninth harmonic of a pulsed Nd:YAG laser) is used to gently ionize the neutral species without fragmentation.[14] The nanosecond pulses of 118-nm light travel parallel to the substrate and through the center of the extraction region of the TOFMS. In the case of positive ionic products, no additional ionization is required. The Ar^+ ion beam is directed normal to the sample.

The experiments are conducted in an ultrahigh vacuum chamber with a typical base pressure of 5×10^{-7} Pa. The chamber pressure rises to 10^{-5} Pa when argon gas is introduced into the ion source but before the introduction of chlorine gas. A chlorine gas background is introduced into the main chamber through a precision leak valve. Chlorine flux to the sample, calculated from the pressure measured with a nude ionization gauge without correction, is varied from 0 to 1.2 of a Cl_2 monolayer per second (ML s^{-1}). The Ar^+ ion beam current ranges between 0.2 and 2 μA at the sample surface depending on the beam energy and source conditions. The full-width at half-maximum beam current, measured with a Faraday cup, corresponds to a beam width of ~0.45 cm. The resulting Ar^+ beam flux is 1.2×10^{-2} ML s^{-1} (μA of current)$^{-1}$. The Ar^+ ion beam is modulated by applying a 1-kHz unsymmetrical square wave with a 200-V amplitude to one of the deflectors. Measurements of the current collected by the 1-cm^2 sample during the application of the deflector voltage establishes that the Ar^+ ion beam is deflected off the sample in approximately 400 ns. These ion pulses of 550 μs duration and 1 kHz repetition rate are used for the experiments.

The Ar^+ ion-enhanced neutral and ionic etch products are mass detected using the TOFMS. The positively charged species are detected by a channel electron multiplier after traveling through a 1-m long flight tube. The positively charged etch products are directly injected into this tube by applying an electrical pulse (between +300 and +500 V) to the spectrometer's repeller plate. This pulse is turned on between 3 and 8 μs after the Ar^+ ion beam is deflected off the sample. The effects of the repeller plate voltage and the delay between the deflection of the ion beam and the repeller pulse on the measurement were examined, and with the exception of changing the absolute intensities, these parameters had little effect on the ion product species observed versus chlorine flux and ion energy. To obtain a mass spectrum of the ionic products, approximately 500 pulses at a 1-kHz rate are averaged on a digital oscilloscope.

Detection of neutral products is more difficult. The ionic products interfere with the detection of the single-photon-ionized neutral products. To eliminate the charged products from the extraction region prior to laser ionization, an additional short voltage pulse (+550 V) is applied first to the extraction grid to eject the charged etch products from the extraction region. A voltage (+400 V) is applied to the repeller plate just before laser ionization. The resulting electrostatic field extracts the products ionized by the 118-nm radiation into the flight tube. The timing and experimental details of this process have been described.[15] Typically, 1000 laser pulses at 10 Hz are required to obtain a spectrum. The larger number of pulses required for the neutral species with respect to the ionic species is a direct result of the approximately 10^3 times greater intensity of the raw signals for the ionic species. Figure 2 shows a typical spectrum of the neutral products. Because the ionization energy of ground-state Ar is greater than the 118-nm radiation, the observation of Ar^+ produced by the 118-nm light in Figure 2

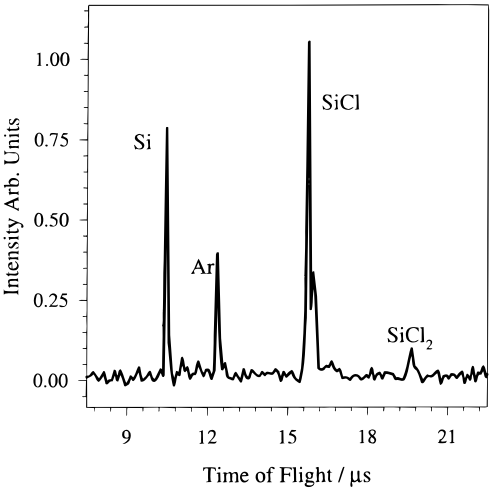

Figure 2. Typical TOFMS spectrum under ion-enhanced etching conditions. The four peaks are assigned to Si, Ar, SiCl, and $SiCl_2$. The presence of Ar indicates the possible production of metastable argon during the sputtering event. The $SiCl_2$ peak is only observed at room temperature and Ar^+ ion energies above 700 eV.

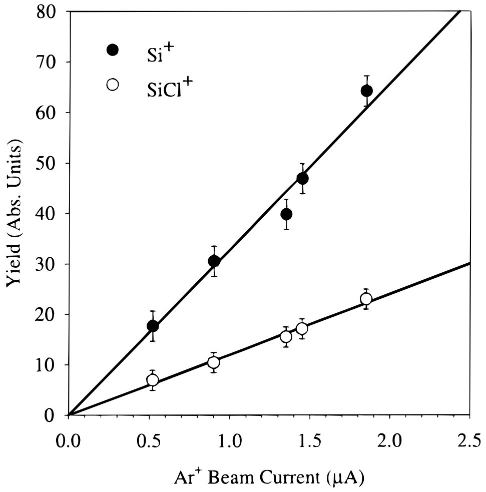

Figure 3. Si^+ and $SiCl^+$ ionic etch product yields plotted versus Ar^+ ion current measured on the sample. A molecular chlorine background pressure was maintained at 4×10^{-4} Pa, and an Ar^+ energy of 975 eV was utilized. Over the range of Ar^+ ion current, the Cl_2 to Ar^+ flux ratio varied from 35 to 140.

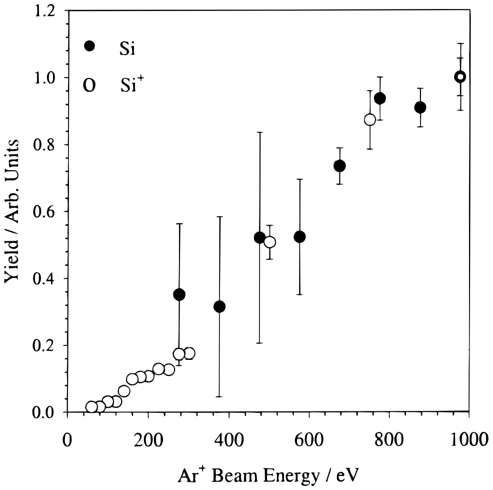

Figure 4. Si neutral and ionic ion-enhanced etch product yields are shown as a function of the kinetic energy of the Ar^+ ion. The yields of the products are normalized so that the value at the highest energy is 1. The Cl_2 flux was maintained at 0.5 ML s^{-1}.

implies the production of metastable, or long-lived, electronically excited neutral Ar atoms during the sputtering event. The weak $SiCl_2$ peak is observed only at room temperature and fluctuates considerably from run to run.

The silicon sample is initially cleaned by sputtering with a 2-keV Ar^+ ion beam followed by high-temperature annealing. The cleanliness is verified by Auger electron spectroscopy. The samples are lightly P-doped (1.2 Ω cm) Si(100) wafers that have been coated on the backside with approximately 300 nm of molybdenum. The edges of the silicon sample are sandwiched between two 25-μm-thick tantalum tabs pressed on by tungsten clamps. The tantalum tabs are then mechanically attached to a copper sample holder. This arrangement is similar to a method previously described.[27]

Results and Discussion

The neutral and ionic etch products are first examined as a function of the ion flux under high chlorine/ion flux ratio conditions. This is followed by measurements of the product distribution and product ratios as a function of the kinetic energy of the Ar^+ ion. Finally, the variations of the neutral and ionic etch products with molecular chlorine flux are presented and discussed. All experiments are performed at room temperature where thermal etching is negligible.

Ion Flux Dependence of the Etch Products. Figure 3 shows a linear dependence of the Si^+ and $SiCl^+$ ionic etch product yields versus beam current measured on the sample. A molecular chlorine background pressure was maintained at 4×10^{-4} Pa. For this measurement, an Ar^+ beam energy of 975 eV was utilized to provide the maximum variation in current. Over the Ar^+ ion current range utilized in Figure 3, the chlorine/ion flux ratio varied from 35 to 140. A similar linear dependence of the neutral etch products as a function of the Ar^+ ion flux, with chlorine/ion flux ratios ≥ 10, has been observed previously for the neutral products.[15] However, under conditions of chlorine/ion flux ratios <10, the rate of production of neutral etch products has been shown to depend on the ratio of chlorine to energetic ions.[12,16] For the neutral product formation under these high flux ratio conditions (chlorine/ion flux ratios ≥ 10), Goodman et al. proposed that the region affected by an ion impact is rechlorinated before a subsequent Ar^+ impact within the same region.[15] This proposed explanation implies that under these conditions the room temperature silicon surface maintains a saturation coverage of chlorine during the ion bombardment.

This interpretation is further supported by the observation here that the yields of the ionic etch products exhibit a linear dependence on the Ar^+ beam current. Because the ions must be produced by direct collision processes,[28] they directly reflect the surface conditions. Although yields of both neutral[15] and ionic etch products are linear functions of the Ar^+ ion flux under high molecular chlorine partial pressures, this result alone does not imply that these products are produced via the same mechanisms. As described below, the linear behavior of the etch products with respect to the ion current will also break down as the chlorine/ion flux ratio is decreased below 10.

Neutral and Ionic Products as a Function of Ion Energy. The yields of neutral and ionic Si and SiCl, plotted as a function of Ar^+ kinetic energy with constant chlorine background pressure, are presented in Figures 4 and 5. The neutral species are recorded at ion energies between 275 and 975 V. A detailed consideration of the relative sensitivities shows that SiCl is by far the dominant product compared to the other observed etch products, Si and $SiCl_2$.[15] For the ionic species, the more sensitive

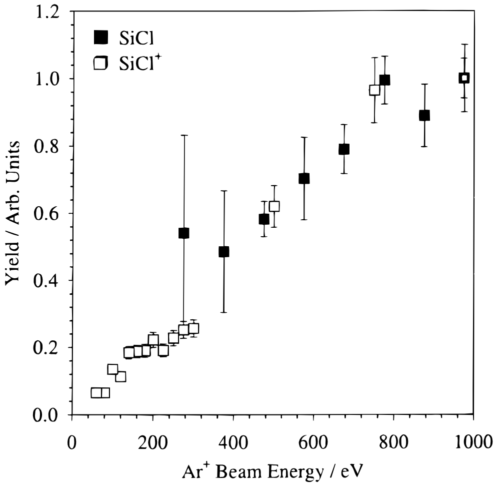

Figure 5. SiCl neutral and ion etch product yields are shown as a function of the kinetic energy of the Ar$^+$ ion. The yields of the products are normalized so that the value at the highest energy is 1. The Cl_2 flux was maintained at 0.5 ML s^{-1}.

detection threshold allows measurements down to 60 eV. To minimize the effect of the changing chlorine/ion flux ratio due to the variation in ion beam current with beam energy, a chlorine/ion flux ratio ≥10 was maintained during these TOFMS measurements. The product intensities were normalized to the ion current at each energy. In addition, each plot is independently normalized to a value of 1 at the highest energy, although it must be noted that the absolute ion yields are expected to be much less than the neutral yields.[28]

No correction is made for possible changes in the velocity distributions of the sputtered particles with changes in the Ar$^+$ ion energy. The average kinetic energy of the sputtered Si and SiCl etch products is expected to be reduced at lower Ar$^+$ kinetic energies. This lower velocity would increase the ion density in the extraction region and enhance the measured signal. Molecular beam measurements show a change in the velocity distribution of the sputtered particle energy from a Maxwell−Boltzmann-like distribution at low energies to a collision-cascade at high energies.[29] Therefore, some caution should be exercised with regard to the quantitative yields shown in Figures 4 and 5 as a function of energy.

The results of Figures 4 and 5 can be qualitatively understood. As the ion energy is increased, more energy is deposited onto the surface and a greater number of neutral and ionic desorption events from the chlorinated surface occur. At energies below 275 eV, the neutral product yields fall below the detection limit. However, the higher detection sensitivity of the ionic products allows measurements down to 60 eV. Total yield measurements show that the energy-dependent decrease in sputter yield varies with $E^{1/2}$ throughout the energy range.[30] There have been very few measurements of the sputter yield below 100 eV;[12,13] however, these measurements show the same functional dependence. Assuming that neutral SiCl is the major product[15] and given both the estimated error bars and the relatively smooth variation of the yield over the 275−1000 eV energy range for the neutral species, the yields shown in Figure 5 for SiCl are consistent with previous measurements.

The rate of ion formation during sputtering need not necessarily follow the neutral product formation. Secondary ions are produced directly during the Ar$^+$ collisions.[28] In contrast, the neutral products can also be formed in postcollision processes by thermal reactions at hot spots generated by the impact or at chemically reactive defects created during bombardment. Over the range of kinetic energies reported here, it is reasonable to assume that the probability of secondary ion formation is approximately independent of energy. At much higher energies, additional ionization pathways are possible. For example, the threshold bombardment energy to generate ions by inner-shell excitations is approximately 4 keV.[28] However, over the range of 60−1000 eV, no additional ionization channels are expected. Thus, it is unlikely that the secondary ion formation probability would rapidly change under the conditions studied. Given this assumption, the similarity between the ionic and neutral etch products suggests that thermal and defect-mediated pathways for the neutrals are minimal, and the results support a direct collision formation mechanism for the Si and SiCl products.

Neutral $SiCl_2$ products can be observed with Ar$^+$ bombardment energies ≥700 eV (see Figure 2); it is possible that even higher kinetic energies are required to desorb the surface species responsible for $SiCl_2$ formation. However, temperature programmed desorption[31] and steady-state thermal etching[14] results suggest that the $SiCl_2$ species is more weakly bound than SiCl. Yet, SiCl is observed at lower Ar$^+$ kinetic energies than $SiCl_2$. In addition, if the production of neutral $SiCl_2$ occurs through a collision mechanism, an ionic $SiCl_2^+$ product should also be observed. However, the ionic $SiCl_2^+$ etch product is not observed, and any possible $SiCl_2^+$ product is below detectable levels. From our calibrations, any possible $SiCl_2^+$ ion signal is less than 1/1000 that of Si$^+$ and less than 1/100 that of SiCl$^+$. In contrast, the neutral $SiCl_2$ signal is approximately 1/10 of the Si and SiCl etch products. The virtual lack of any appreciable flux of the $SiCl_2^+$ ion implies that the neutral $SiCl_2$ product is possibly formed by a different mechanism than that responsible for the Si and SiCl etch products. Subsequent thermal reactions at defect sites are one possibility. In this case, the $SiCl_2^+$ product would not necessarily be generated in conjunction with the neutral $SiCl_2$. At higher Ar$^+$ bombardment energies, a larger number of such sites are formed.

The possible importance of thermal reactions at defect sites for the formation of $SiCl_2$ has important ramifications for MD studies, which typically follow the reaction only out to several picoseconds after the collision. One MD study of atomic layer etching of silicon estimated the time scale for the postcollision generation of these products during simultaneous exposure to neutral species and ion beams to be on the order of hundreds of milliseconds.[32] Some progress has been made to better simulate these processes during ion-enhanced etching. The MD simulation by Barone et al. utilized a first-order thermal desorption rate expression to approximate desorption events at longer times than the simulation time of 1.2 ps.[22] In addition, a recent study by Hanson et al. examined the effect of background atomic chlorine on the mechanisms of product formation.[25]

Neutral and Ionic Si to SiCl Product Ratios. Further information can be gained from the changes in the SiCl/Si and SiCl$^+$/Si$^+$ intensity ratios as a function of Ar$^+$ ion energy. The ratios calculated from the intensities shown in Figures 4 and 5, uncorrected for particle velocities, are plotted versus the ion beam energy in Figure 6. Because the intensities of the neutral and ionic products are normalized to 1 at the highest energy, the neutral and ionic ratios are equal to 1 at the highest energy. No additional normalization is applied to the data. Both neutral and ionic ratios of SiCl/Si increase with decreasing primary ion beam energy. These ratios will depend on the coverage of the various singly and multiply chlorinated silicon surface species and the differences between their surface binding energies. The results show that either the saturation chlorine coverage increases with decreasing beam energy or that, as the energy provided

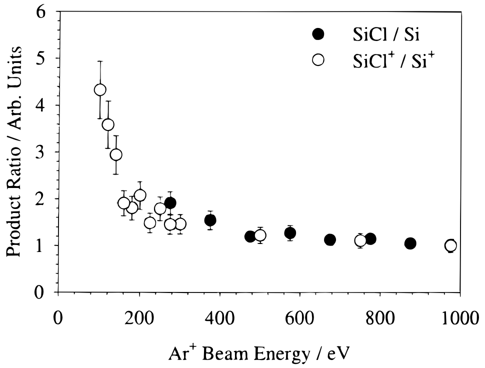

Figure 6. SiCl/Si and SiCl$^+$/Si$^+$ product yield ratios are plotted versus the kinetic energy of the Ar$^+$ ion. The Cl$_2$ flux was maintained at 0.5 ML s^{-1}.

by the Ar$^+$ ions is decreased, there is a preference for the desorption of more weakly bound SiCl species. An argument can be considered based on the changing penetration depth of the Ar$^+$ ion. However, MD studies of Si(100) sputtered with 1 keV Ar$^+$ ions have shown that while the openness of the Si(100) surface allows the first four layers to be clearly visible to the incident Ar$^+$ ion, 98% of the Si products detected come from only the first three layers.[33] Thus, a mechanism based on changing penetration depths is unlikely.

At energies less than approximately 400 eV, the amount of chlorinated product with respect to the atomic etch product seems to increase much more rapidly. This effect is clearly seen in the ionic product ratio because these measurements are possible at much lower energies. The possible changes in the relative velocity distribution between the Si and SiCl discussed above may be responsible for some of this more rapid increase in the product ratios. However, the large increase also supports a rapid increase in amount of chlorinated species on the surface. Evidence for the latter explanation comes from the MD simulation by Hanson et al. over an energy range from 50 to 200 eV,[25] which also indicates an increasing flux of desorbed chlorinated species with decreasing energy. These observations suggest that there is a clear difference in the sputtering mechanisms that occur at lower ion beam energies. Additional experimental studies of the etch products are clearly required to connect the large volume of work in the keV range (see Table 1) to the lower energy studies. Only recently have there been several total yield studies of Ar$^+$ ion-enhanced etching with molecular chlorine and ion beam energies less than 200 eV.[12,13]

Molecular Chlorine Flux Dependence. Varying the chlorine/Ar$^+$ ion flux from 0 to 10 allows for the examination of the sputtering processes as the surface transforms from a clean silicon surface to a chlorinated silicon surface at saturation coverages. Under conditions of constant ion flux, the chlorine coverage will depend only on the chlorine flux to the surface. Figure 7A shows the measured Cl$_2$ pressure dependence for the Si and Si$^+$ etch products with an Ar$^+$ ion energy of 975 eV. Figure 7B shows similar results for the SiCl and SiCl$^+$ etch products also at an Ar$^+$ energy of 975 eV. Because absolute yields are unknown, the neutral and ionic products are scaled to provide the best relative fit between the variations of both products with the Cl$_2$ pressure. In addition, the variation of the ionic product signals with chlorine flux observed at 200 eV is found to be very similar to the variations at 975 eV.

Reaction kinetics of ion-enhanced etching were previously examined by measurement of the product yields as a function of chlorine pressure with constant ion flux.[15] Goodman et al. proposed a simple kinetic model for the formation of both neutral Si and SiCl ion-enhanced etch products based on the neutral chlorine/ion flux product dependence.[15] This model takes into account various differences between the Si and the SiCl etch products and is similar to ones proposed by Backer et al.[34] and Levinson et al.[13] The observed similarity between the neutral and the ionic species as a function of molecular chlorine flux suggests that the neutral and the ionic etch products are created by similar mechanisms.

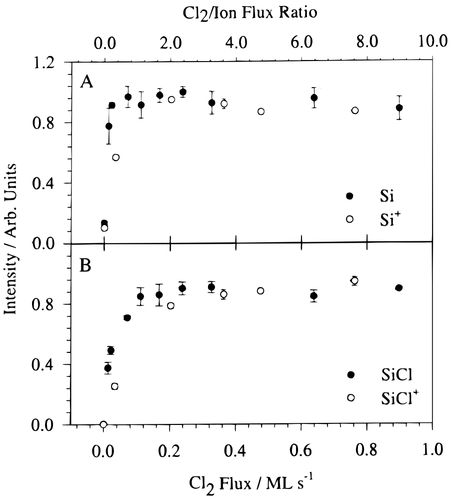

Figure 7. Cl$_2$ background pressure dependence of (A) Si and Si$^+$ product yields and (B) SiCl and SiCl$^+$ product yields are shown. These data are collected with an Ar$^+$ energy of 975 eV and flux of 0.01 ML s^{-1}.

For the neutral SiCl product (see Figure 7), the yield initially increases rapidly from zero to almost its maximum value with increasing molecular chlorine flux. After this rapid rise, the yield increases much more slowly with increasing pressure. This behavior is explained by a simple kinetic model based on two reactions. One reaction is the adsorption of molecular chlorine on free silicon surface sites to yield a chlorinated precursor. The other involves the collisional removal of this precursor to form a chlorinated etch product and to generate additional free silicon surface sites.[15] The collisional removal of a surface precursor is further supported by the similarities of the neutral and ionic SiCl etch products.

The variation with Cl$_2$ pressure shown in Figure 7 for neutral Si can also be qualitatively understood. A detailed analysis over a wider range of pressures and ion energies has been presented for the neutral Si species.[15] Goodman et al. found that the generation of the atomic Si species was more complex than that of the SiCl product.[15] The ejected Si product can arise from both physical sputtering of unreacted areas of the Si surface and chemical sputtering from a chlorinated silicon precursor. In addition, Si produced from chemical sputtering has a much higher detection probability than that from physical sputtering, possibly due to the different velocity distributions imparted to the Si product.[15] Initially, the Si yield is composed of physically sputtered Si. With the introduction of Cl$_2$, there is a rapid increase in yield due to the formation of chemically sputtered Si, which may indicate it is detected more efficiently than the physically sputtered Si. The yield increases to a maximum value. Following this maximum, a slow decrease in the neutral Si yield occurs. By careful fitting of the atomic Si yields versus molecular chlorine over an extensive range of molecular chlorine flux and at several different Ar$^+$ ion energies, the decrease has been ascribed to the increasingly chlorinated silicon surface.[15] This decrease results in a reduction in the atomic Si product in favor of the more chlorinated etch products.[15]

Conclusions

Neutral and ionic silicon etch products that are evolved during Ar^+ ion-enhanced etching of room temperature Si(100) with molecular chlorine are measured using TOFMS. The yields of neutral and ionic etch products are examined as a function of ion energy, ion flux, and molecular chlorine flux. The neutral product yields are measured over an Ar^+ ion energy range of 275−975 eV, while the ionic product measurements start at 975 and continue down to 60 eV. For the neutral etch products, the Si and SiCl species dominate the TOFMS spectra with a minor contribution of $SiCl_2$ at the higher Ar^+ ion kinetic energies. For the positively charged ionic etch products, only Si^+ and $SiCl^+$ are observed. In addition, the yield of each product increases with increasing ion energy. Although neutral $SiCl_2$ products can be observed at Ar^+ bombardment energies above 700 eV, the ionic $SiCl_2{}^+$ product is not observed. It is possible that the neutral $SiCl_2$ product is formed by subsequent thermal reactions. This result has important implications for MD studies. In addition, an apparently rapid increase in the SiCl/Si and the $SiCl^+/Si^+$ product ratios at approximately 400 eV occurs. A propensity for increasingly chlorinated etch products is possible as the Ar^+ ion kinetic energy decreases.

The Cl_2 flux, energy, and current dependencies of the neutral and the ionic products show clear similarities to those predicted by a previously proposed model that describes the formation of neutral Si and SiCl etch products based on product formation by direct collisions.[15] Under a molecular chlorine background and Cl_2/Ar^+ flux ratios <200, a direct collisional mechanism is currently the best explanation for the experimental data presented here and in ref 15. The observation that the ion products follow the neutral products supports this assumption, since the ionic products must be directly produced. Additional theoretical modeling will provide more insight. One clear challenge for the MD simulations is the influence of the molecular chorine background on the surface processes. In addition, these simulations should be extended to higher energies (>200 eV) to allow better comparison with experiments. Similarly, the challenge for experimental studies is the determination of the etch products at lower Ar^+ ion energy (<200 eV) and higher Cl_2/Ar^+ flux ratios.

Acknowledgment. N.M. would like to acknowledge experience during his graduate studies gained under the guidance of G. A. Somorjai. The authors would like to acknowledge the expert help of the JILA Instrument Shop. They gratefully acknowledge support of this work by the U.S. Army Research Office, Physics Division. Additional equipment and support were provided by the National Science Foundation and the National Institute of Standards and Technology.

References and Notes

(1) Suzuki, K.; Itabashi, N. *Pure Appl. Chem.* **1996**, *68*, 1011.
(2) Flamm, D. L. *Pure Appl. Chem.* **1990**, *62*, 1709.
(3) Donnelly, V. M.; Flamm, D. L. *Solid State Technol.* **1981**, *24*, 161.
(4) Hamers, R. J.; Wang, Y. J. *Chem. Rev.* **1996**, *96*, 1261.
(5) Engel, T. *Jpn. J. Appl. Phys., Part 1* **1996**, *35*, 2403.
(6) Leone, S. R. *Jpn. J. Appl. Phys., Part 1* **1995**, *34*, 2073.
(7) Waltenburg, H. N.; Yates, J. T., Jr. *Chem. Rev.* **1995**, *95*, 1589.
(8) Rhodin, T. *Prog. Surf. Sci.* **1995**, *50*, 131.
(9) Winters, H. F.; Coburn, J. W. *Surf. Sci. Rep.* **1992**, *14*, 161.
(10) Yu, M. L.; DeLouise, L. A. *Surf. Sci. Rep.* **1994**, *19*, 285.
(11) Zalm, P. C. *Vacuum* **1986**, *36*, 787.
(12) Chang, J. P.; Arnold, J. C.; Zau, G. C. H.; Shin, H.-S.; Sawin, H. H. *J. Vac. Sci. Technol., A* **1997**, *15*, 1853.
(13) Levinson, J. A.; Shaqfeh, E. S. G.; Balooch, M.; Hamza, A. V. *J. Vac. Sci. Technol., A* **1997**, *15*, 1902.
(14) Materer, N.; Goodman, R. S.; Leone, S. R. *J. Vac. Sci. Technol., A* **1997**, *15*, 2134.
(15) Goodman, R. S.; Materer, N.; Leone, S. R. *J. Vac. Sci. Technol.,* A **1999**, *17*, 3340.
(16) Coburn, J. W. *J. Vac. Sci. Technol., B* **1994**, *12*, 1384.
(17) Kolfschoten, A. W.; Haring, R. A.; Haring, A.; de Vries, A. E. *J. Appl. Phys.* **1984**, *55*, 3813.
(18) McNevin, S. C.; Becker, G. E. *J. Vac. Sci. Technol., B* **1985**, *3*, 485.
(19) van Zwol, J.; van Laar, J.; Kolfschoten, A. W.; Dieleman, J. *J. Vac. Sci. Technol., B* **1987**, *5*, 1410.
(20) Barker, R. A.; Mayer, T. M.; Pearson, W. C. *J. Vac. Sci. Technol., B* **1983**, *1*, 37.
(21) Rossen, R. A.; Sawin, H. H. *J. Vac. Sci. Technol., A* **1987**, *5*, 1595.
(22) Barone, M. E.; Graves, D. B. *J. Appl. Phys.* **1995**, *78*, 6604.
(23) Feil, H.; Dieleman, J.; Garrison, B. J. *J. Appl. Phys.* **1993**, *74*, 1303.
(24) Kubota, N. A.; Economou, D. J.; Plimpton, S. J. *J. Appl. Phys.* **1998**, *83*, 4055.
(25) Hanson, D. E.; Voter, A. F.; Kress, J. D. *J. Appl. Phys.* **1997**, *82*, 3552.
(26) Wiley, W. C.; McLaren, I. H. *Rev. Sci. Instrum.* **1955**, *26*, 1150.
(27) Koehler, B. G.; Mak, C. H.; Arthur, D. A.; Coon, P. A.; George, S. M. *J. Chem. Phys.* **1988**, *89*, 1709.
(28) Yu, M. L. In *Sputtering by Particle Bombardment III*; Behrish, R., Wittmaack, K., Eds.; Springer-Verlag: Berlin, Heidelberg, 1991; p 91.
(29) Oostra, D. J.; Haring, A.; van Ingen, R. P.; de Vries, A. E.; van Veen, G. N. A. *J. Appl. Phys.* **1988**, *64*, 315.
(30) Steinbruchel, C. *Appl. Phys. Lett.* **1989**, *55*, 1960.
(31) Szabo, A.; Farrall, P. D.; Engel, T. *Surf. Sci.* **1994**, *312*, 284.
(32) Athavale, S. D.; Economou, D. J. *J. Vac. Sci. Technol., A* **1995**, *13*, 966.
(33) Smith, R.; Harrison, D. E., Jr.; Garrision, B. J. *Phys. Rev. B* **1989**, *40*, 93.
(34) Backer, R. A.; Mayer, T. M.; Pearson, W. C. *J. Vac. Sci. Technol., B* **1983**, *1*, 37.
(35) Sanders, F. H. M.; Kolfschoten, A. W.; Dieleman, J.; Haring, R. A.; Haring, A.; de Vries, A. E. *J. Vac. Sci. Technol., A* **1984**, *2*, 487.